

On the Capacity of Bandlimited Optical Intensity Channels with Gaussian Noise

Jing Zhou and Wenyi Zhang, *Senior Member, IEEE*

Abstract—We determine lower and upper bounds on the capacity of bandlimited optical intensity channels (BLOIC) with white Gaussian noise. Three types of input power constraints are considered: 1) only an average power constraint, 2) only a peak power constraint, and 3) an average and a peak power constraint. Capacity lower bounds are derived by a two-step process including 1) for each type of constraint, designing admissible pulse amplitude modulated input waveform ensembles, and 2) lower bounding the maximum achievable information rates of the designed input ensembles. Capacity upper bounds are derived by exercising constraint relaxations and utilizing known results on discrete-time optical intensity channels. We obtain degrees-of-freedom-optimal (DOF-optimal) lower bounds which have the same pre-log factor as the upper bounds, thereby characterizing the high SNR capacity of BLOIC to within a finite gap. We further derive intersymbol-interference-free (ISI-free) signaling based lower bounds, which perform well for all practical SNR values. In particular, the ISI-free signaling based lower bounds outperform the DOF-optimal lower bound when the SNR is below 10 dB.

Index Terms—Bandlimited channel, channel capacity, intensity modulation, optical wireless communications.

I. INTRODUCTION

A. Background and Related Work

INTENSITY modulation and direct detection (IM/DD) is widely used in optical communications. In IM/DD, information is conveyed by the varying intensity of transmitted optical signal, and the receiver detects the intensity of the received signal. There have been extensive studies on design and realization of IM/DD based optical wireless communication systems (see [1], [2] and references therein). This paper focuses on a simplified IM/DD channel model, known as the optical intensity channel with Gaussian noise. This model is suitable for some kinds of IM/DD systems, e.g., indoor free space optical communications [1], [3]. In optical intensity channels, typically the average and/or peak optical power is constrained¹ due to safety reasons and practical considerations.

This work was supported in part by the National Key Basic Research Program of China under Grant 2013CB329205, by the National Natural Science Foundation of China under Grant 61379003, and by the Fundamental Research Funds for the Central Universities under Grants WK2100060020 and WK3500000003.

Jing Zhou is with the Department of Electronic Engineering and Information Science, University of Science and Technology of China, Hefei, China, and with the Air Force Aviation University, Zibo, China (e-mail: jzee@ustc.edu.cn).

Wenyi Zhang is with the Key Laboratory of Wireless-Optical Communications, Chinese Academy of Sciences, and with the Department of Electronic Engineering and Information Science, University of Science and Technology of China, Hefei, China (e-mail: wenyizha@ustc.edu.cn).

¹Since the optical intensity is the optical power transferred per unit area, a constraint on optical power is also a constraint on intensity. In this paper we use ‘power’ to refer to the optical power unless otherwise specified.

Therefore the optical intensity channel we considered has two fundamental differences with electrical channel models like the classical AWGN channel: 1) a nonnegativity constraint on the input signal, 2) a different input cost metric. It is clear that typical signaling methods for electrical channels cannot be applied directly in optical intensity channels because of these differences.

A number of information theoretic studies on optical intensity channels have been reported, mostly on discrete-time optical intensity channels (DTOIC); see, e.g., [3]–[8]. For DTOIC with only an average power constraint, the exact capacity is still unknown, whereas tight upper and lower bounds have been established. When the input is further bounded from above due to a peak power constraint, the optimal input distribution and the capacity can be numerically computed [9], [10]. Moreover, recent works have provided systematic results on capacity-achieving input design for DTOIC [5], [7]. Only a few information theoretic studies have considered continuous-time optical intensity channel models. In [11], sphere packing based capacity upper bounds for multicarrier optical intensity channels (MCOIC) were established. Capacity bounds for bandlimited optical intensity channels (BLOIC) with an average power constraint were studied in [3]. In another aspect, the design of ISI-free signaling over BLOIC was studied in [12]–[14], while the information rate was not considered therein.

B. Channel Model and Motivation of Our Study

The BLOIC model considered in this paper is

$$Y(t) = X(t) + Z(t), \quad X(t) \geq 0 \quad (1)$$

where $X(t)$ is bandlimited to $\mathcal{W} \triangleq [-W, W]$, $Z(t)$ is white Gaussian noise (the definition follows that in [15]) of one-sided power spectral density N_0 with respect to \mathcal{W} . The bandwidth constraint of BLOIC is due to the optoelectronic components and multipath distortion [1], [3]. In (1), without loss of generality we set the channel gain (including, e.g., the responsivity of the photodiode and the optoelectronic conversion factor in IM/DD systems) to be unity, as in [3], [4]. The DTOIC

$$Y[n] = X[n] + Z[n], \quad X[n] \geq 0 \quad (2)$$

is the discrete-time analog of (1), where $Z[n] \sim \mathcal{N}(0, \sigma^2)$ ($\mathcal{N}(a, b)$ denotes Gaussian distribution with mean a and variance b) is independent and identically distributed (i.i.d.).

To model the input constraint, we define the instantaneous powers as $\mathcal{P}(X(t)) = x(t)$ and $\mathcal{P}(X[n]) = x[n]$ for BLOIC

and DTOIC, respectively. These definitions are different from those of the electrical power which is proportional to the squared amplitude of the signal. Then the average power is $E[X[n]]$ in DTOIC. In BLOIC, the average power is defined as

$$\mathcal{P}_{\{X\}} = \lim_{T \rightarrow \infty} \frac{1}{2T} E \left[\int_{-T}^T X(t) dt \right]. \quad (3)$$

Here we follow the definition of [15, Definition 14.6.1].

For most classical channels such as the AWGN channel, the linear Gaussian channel or fading channels, we have the following relationship between the capacity of the continuous-time bandlimited channel model and its discrete-time analog with the same signal-to-noise ratio:

$$C_{BL} = C_{DT} \cdot 2W \text{ transmissions per second.} \quad (4)$$

This relationship can be established by orthogonal transforms, e.g., by Nyquist rate signaling/sampling or more rigorously by Karhunen-Loève expansion and the 2WT theorem.² Moreover, signaling schemes designed based on discrete-time models can be directly utilized in bandlimited communications by simple modulation/demodulation methods. Because of these facts, many studies based on classical channels reasonably consider only the discrete-time channel models, where the relationship between the discrete-time channel inputs (i.e. $x[n]$) and the continuous-time signal they represent (i.e. $x(t)$) is

$$x(t) = \sum_n x[n] \frac{\sin \pi(2Wt - n)}{\pi(2Wt - n)}. \quad (5)$$

However, in this paper we emphasize that the aforementioned equivalent relationship does not hold between DTOIC and BLOIC. According to (5), it is easy to verify that the equivalent bandlimited waveform of a given nonnegative input sequence is not necessarily nonnegative everywhere. In other words, it is possible that an admissible input sequence in DTOIC corresponds to an inadmissible input waveform in BLOIC.³ Then it is clear that the capacity of BLOIC can not be obtained by solving the capacity problem of DTOIC and using (4). Therefore, when a bandwidth constraint exists, using DTOIC as the model of a continuous-time optical intensity channel is an *oversimplification* of the capacity problem.

To the best of our knowledge, [3] is the only information theoretic study directly on the BLOIC model (1). This study is restricted to time-disjoint signaling (TDS) based on a finite (typically low) dimensional signal space model over a finite time interval. Using that model, the continuous-time channel is converted to a discrete-time vector Gaussian channel and the input nonnegativity constraint is correspondingly converted to an admissible region in the signal space. Capacity bounds are derived based on the converted vector Gaussian channel with the admissible input region. It is thus clear that the upper bounds obtained therein are only information rate upper

bounds of specific TDS schemes, rather than capacity upper bounds for the BLOIC. Moreover, due to the finite time length of the signal space model, the bandwidth constraint can only be approximately satisfied by permitting an ϵ -fractional out-of-band energy. Since the bandwidth is sensitive to ϵ , varying ϵ causes the achievable spectral efficiency to vary significantly. When ϵ tends to zero the achievable spectral efficiency tends to zero. Even for a fixed ϵ and given bandwidth, the signaling rate is limited due to the poor time-frequency concentration of the rectangular basis function needed in the BLOIC signal space model. So the available DOFs of the bandlimited channel is hardly exploited in the most efficient way.

C. Our Contribution

In this paper, we study the fundamental limits of communication over the BLOIC under different types of input constraints. By designing admissible pulse amplitude modulated (PAM) input waveform ensembles with i.i.d. input symbols and lower bounding their maximum achievable information rates, we derive two kinds of capacity lower bounds: the DOF-optimal lower bounds and the ISI-free signaling based lower bounds. The DOF-optimal lower bounds achieve the optimal pre-log factor of the channel capacity by comparing with capacity upper bounds derived from constraint relaxation. Thus we characterize the high-SNR capacity of the BLOIC to within a finite gap. For example, the high-SNR asymptotic gap between the tightest lower and upper capacity bounds for the only average power constrained case is 4.34 dB in SNR. The ISI-free signaling is preferred in practical communication systems because of its low detection complexity. We show that the ISI-free signaling based lower bounds perform well for all practical SNR values, especially for low to moderate SNR. At high SNR, introducing a direct current (DC) bias in the signal design is shown to be very helpful for boosting the information rate. We also study the effects of different peak-to-average-power ratios and different types of modulation pulses (i.e. shaping filters) on the capacity lower bounds, and give several conjectures and discussions. All these results provide understanding on fundamental limits and signaling scheme design for bandlimited communications using IM/DD.

The remaining part of the paper is organized as follows. Section II presents our methods and main results. Section III gives comparisons among the capacity bounds based on numerical results. Section IV provides some discussions and two conjectures.

Throughout the paper the following notations are used: $p_X(x)$ denotes the probability density function (PDF) of X ; $h(\cdot)$ stands for the differential entropy, i.e. $h(X) = -\int_{-\infty}^{\infty} p_X(x) \log p_X(x) dx$; $I(\mathbf{Q}, \mathbf{V}) \triangleq I(X; Y)$ stands for the mutual information between input X and output Y of a channel with transition probability measure \mathbf{V} when X has distribution \mathbf{Q} ; $\mathcal{H}[X(t)]$ stands for the differential entropy per DOF of the bandlimited waveform ensemble $X(t)$; $\mathcal{I}[X(t); Y(t)]$ stands for the mutual information per DOF between two bandlimited waveform ensembles $X(t)$ and $Y(t)$; C_A^B denotes the capacity of channel A under constraint B; \mathcal{R}_A^B denotes the maximum achievable information rate of a

²See [16], [17]. The 2WT theorem says that a channel with bandwidth W has essentially $2WT$ degrees of freedom (DOFs) in a length- T time interval, where $T \gg 1/W$ and DOF is defined as the dimension of the signal space in that time interval.

³Note that the inadmissible waveforms can always be avoided in practice by proper engineering design, but at the expense of performance, as shown later.

TABLE I
ABBREVIATIONS

AP	Average power
BLAWGN	Bandlimited AWGN
BLOIC	Bandlimited optical intensity channel
DC	Direct current
DOF	Degrees of freedom
DTAWGN	Discrete-time AWGN
EPI	Entropy power inequality
IM/DD	Intensity modulation and direct detection
i.i.d.	Independent and identically distributed
ISI	Intersymbol interference
MCOIC	Multicarrier optical intensity channel
PAM	Pulse amplitude modulation
PAPR	Peak-to-average-power-ratio
PC	Power constraint
PDF	Probability density function
PL pulse	Parametric linear pulse
PNR	Peak-to-noise ratio
PP	Peak power
PSWF	Prolate spheroidal wave function
SC pulse	Spectral-cosine pulse
SNR	Signal-to-noise ratio
TDS	Time-disjoint signaling

constrained signaling scheme B over channel A. Boldface is used to denote matrices and vectors. Table I lists some abbreviations used in this paper.

II. METHODS AND RESULTS

A. Preliminaries and Basic Methods

The different input power constraints in the BLOIC considered in this paper are given in Table II. We use r to denote the peak-to-average-power-ratio (PAPR), which is the ratio of the maximum allowed peak power (PP) to the maximum allowed average power (AP). We further use PC as a general notation for these power constraints when a general discussion on them is needed. We denote a BLOIC under AP constraint as AP-BLOIC, and so on. For the DTOIC and the BLAWGN channel similar notations are used.

In a bandlimited channel the input and output are random waveforms, while the input is drawn from a given waveform ensemble. Following Shannon [18], we define the entropy per DOF of an input ensemble $X(t)$ through the distribution of its Nyquist sample sequence as

$$\mathcal{H}[X(t)] = \lim_{N \rightarrow \infty} \frac{1}{2N+1} \int p_{\mathbf{X}}(\mathbf{x}) \log \frac{1}{p_{\mathbf{X}}(\mathbf{x})} d\mathbf{x} \quad (6)$$

TABLE II
DIFFERENT INPUT POWER CONSTRAINTS IN BLOIC

Power Constraint	Definition
AP	$\mathcal{P}_{\{X\}} \leq \mathcal{E}, 0 \leq x(t) \leq \infty$
PP	$0 \leq x(t) \leq \mathcal{A}$
PAPR	$\mathcal{P}_{\{X\}} \leq \mathcal{E}, 0 \leq x(t) \leq r\mathcal{E}$

where $\mathbf{X} = X_{-N}, \dots, X_0, \dots, X_N$ is the Nyquist sample sequence of $X(t)$. For example, for $Z(t)$ defined in (1) we have $\mathcal{H}[Z(t)] = \log \sqrt{2\pi e N_0 W}$. The capacity of a bandlimited channel with input ensemble $X(t)$ and output $Y(t)$ is defined as

$$\mathcal{C} = 2W \cdot \max_{p_{\mathbf{X}}(\mathbf{x})} \mathcal{I}[X(t); Y(t)] \quad (7)$$

where $\mathcal{I}[X(t); Y(t)]$ is the mutual information per DOF between $X(t)$ and $Y(t)$:

$$\begin{aligned} \mathcal{I}[X(t); Y(t)] &= \lim_{N \rightarrow \infty} \frac{1}{2N+1} \iint p_{\mathbf{X}, \mathbf{Y}}(\mathbf{x}, \mathbf{y}) \log \frac{p_{\mathbf{X}, \mathbf{Y}}(\mathbf{x}, \mathbf{y})}{p_{\mathbf{X}}(\mathbf{x})p_{\mathbf{Y}}(\mathbf{y})} d\mathbf{x}d\mathbf{y}, \end{aligned} \quad (8)$$

where $\mathbf{X} = X_{-N}, \dots, X_0, \dots, X_N$ and $\mathbf{Y} = Y_{-N}, \dots, Y_0, \dots, Y_N$, which are the Nyquist samples of $X(t)$ and $Y(t)$, respectively. The maximum achievable information rate \mathcal{R} of a specific signaling scheme has the same definition as \mathcal{C} except that the input ensemble $X(t)$ must be generated using that signaling scheme.

Our achievability results (lower bounds) for the BLOIC are derived by two basic steps:

- 1) Designing an admissible input waveform ensemble satisfying certain constraints.
- 2) Lower bounding the maximum achievable information rate of the designed input ensemble.

In particular, we design PAM input ensembles with i.i.d. input symbols as

$$X_{\text{PAM}}(t) = \sum_i X_i g(t - iT_s), \quad X_{\text{PAM}}(t) \geq 0 \quad (9)$$

to accomplish the first step, where the modulation pulse $g(t)$ is a real \mathcal{L}_2 function (i.e. a finite-energy signal) bandlimited to \mathcal{W} . The design includes reasonable choices of the symbol rate $1/T_s$, the input symbol distribution $p_X(x)$, and the pulse $g(t)$.

Table III lists the pulses used in our results, including the sinc pulse, the S2 pulse [13], the spectral-cosine (SC) pulse, and the (first order) parametric linear (PL) pulse [19] (the definition of parameters \mathcal{S}_N and \mathcal{G} will be given in (13)–(15)). Fig. 1 shows the Fourier transform of these pulses. To simplify the proof of results we normalize the sinc, the S2, and the SC pulses to make them satisfy

$$\int_{-\infty}^{\infty} g(t) dt = \frac{1}{2W}, \quad (10)$$

and normalize the PL pulse to make it satisfy the following definition.

TABLE III
LIST OF THE PULSES USED

Name	Notation and Definition	Remarks
Sinc	$g_{\text{sinc}}(t) = \text{sinc}(2Wt) = \frac{\sin 2\pi Wt}{2\pi Wt}$	$S_N = \infty, \mathcal{G} = 1$
S2	$g_{\Delta}(t) = \frac{1}{2} (\text{sinc}(Wt))^2 = \frac{\sin^2 \pi Wt}{2(\pi Wt)^2}$	$S_N = 1, \mathcal{G} = \frac{1}{e^2}$
SC	$g_{\cos}(t) = \text{sinc}(2Wt - \frac{1}{2}) + \text{sinc}(2Wt + \frac{1}{2}) = \frac{2 \cos 2\pi Wt}{\pi(1-16W^2t^2)}$	$S_N = \frac{4}{\pi}, \mathcal{G} = \frac{1}{4}$
PL	$g_{\text{PL}}(t) = \text{sinc}\left(\frac{2Wt}{1+\beta}\right) \text{sinc}\left(\frac{2\beta Wt}{1+\beta}\right) = \frac{\sin\left(\frac{1+\beta}{1+\beta} 2\pi Wt\right) \sin\left(\frac{\beta}{1+\beta} 2\pi Wt\right)}{\beta \left(\frac{2\pi Wt}{1+\beta}\right)^2}, \beta \in (0, 1]$	

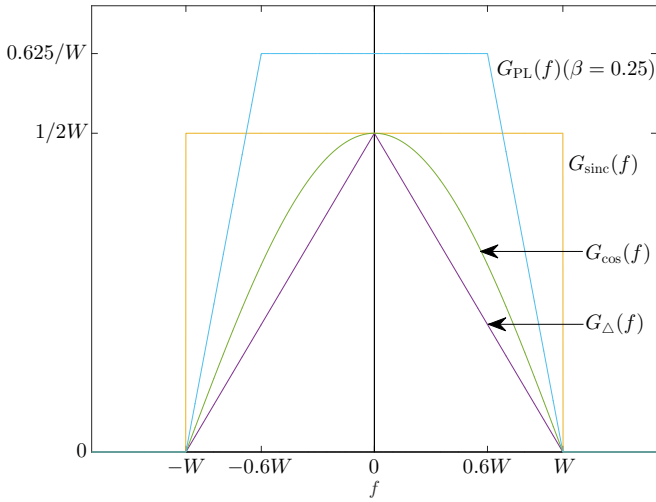


Fig. 1. The Fourier transforms of the pulses used.

Definition 1: A normalized Nyquist pulse $g_{\beta}(t)$ with roll off factor β is a real \mathcal{L}_2 function which is bandlimited to \mathcal{W} and satisfies

$$g_{\beta}(nT_0) = \delta[n] \quad (11)$$

where $T_0 = \frac{1+\beta}{2W}$, and $\delta[n]$ is the unit impulse.

Note: Letting $G_{\beta}(f)$ be the Fourier transform of $g_{\beta}(t)$, it is easy to show that $G_{\beta}(f)$ satisfies

$$G_{\beta}(0) = \int_{-\infty}^{\infty} g_{\beta}(t) dt = T_0. \quad (12)$$

Our lower bounds can be categorized as DOF-optimal lower bounds and ISI-free signaling based lower bounds, which are given in Sec. II-B and Sec. II-C, respectively. The basic idea for deriving DOF-optimal lower bounds is due to Shannon's derivation of capacity bounds for PP-BLAWGN channel in his 1948 landmark paper [18]. The ISI-free signaling based lower bounds are derived by designing admissible ISI-free signaling schemes and considering the capacity of the equivalent discrete-time memoryless channel models.

We will present some general lower bounds which holds for all $g(t)$ or $p_X(x)$ satisfying certain constraints, and then use some specific $g(t)$ or $p_X(x)$ to get specific lower bounds.

Some of the general lower bounds are given with respect to two parameters which are

$$\mathcal{G} \triangleq \exp\left(\frac{1}{W} \int_0^W \log |2W \cdot G(f)|^2 df\right), \quad (13)$$

$$\mathcal{S}(\tau) \triangleq \max_{t \in [0, \tau]} \sum_{i=-\infty}^{\infty} |g(t - i\tau)|, \quad (14)$$

where $G(f)$ is the Fourier transform of $g(t)$. General lower bounds of this flavor were introduced for the PP-BLAWGN channel in [20], where Shannon's 1948 lower bound was tightened by optimizing the modulation pulse used. For brevity we further define

$$S_N \triangleq \mathcal{S}\left(\frac{1}{2W}\right), \quad S_{\beta} \triangleq \mathcal{S}\left(\frac{1+\beta}{2W}\right). \quad (15)$$

The converse results are given in Sec. II-D, where the bounding technique used is also based upon [18].

B. DOF-Optimal Capacity Lower Bounds

The following lemma from [18] plays a crucial role in deriving the results in this subsection.

Lemma 1: If an ensemble of waveform $X_I(t)$ bandlimited to \mathcal{W} is filtered by $G(f)$, then the entropy per DOF of the output ensemble is

$$\mathcal{H}[X_O(t)] = \mathcal{H}[X_I(t)] + \frac{1}{2W} \int_0^W \log |G(f)|^2 df. \quad (16)$$

Proof: See [21, Chapter 6.4]. ■

All the results in this subsection are derived using i.i.d. Nyquist rate input ensembles as

$$X_{\text{PAM}}(t) = \sum_i X_i g\left(t - \frac{i}{2W}\right), \quad X_{\text{PAM}}(t) \geq 0. \quad (17)$$

A symbol rate no less than the Nyquist rate is necessary to exploit all the available DOFs of bandlimited channels in the high SNR regime [22].

Lemma 2: The maximum achievable information rate achieved by the i.i.d. Nyquist rate ensemble $X_{\text{PAM}}(t)$ in (17) transmitted over the BLOIC can be lower bounded by

$$\mathcal{R}_{\text{PAM}} \geq W \log \left(1 + \frac{\mathcal{G} \exp(2h(X))}{2\pi e N_0 W}\right) \quad (18)$$

where \mathcal{G} is defined as (13).

Proof: Consider an ergodic or cyclostationary ensemble of waveform $X(t)$ bandlimited to \mathcal{W} . For an additive noise channel bandlimited to \mathcal{W} the information rate

$$\begin{aligned}\mathcal{R} &= 2W \cdot \mathcal{I}[X(t); Y(t)] \\ &= 2W \cdot (\mathcal{H}[Y(t)] - \mathcal{H}[Y(t)|X(t)]) \\ &= 2W \cdot (\mathcal{H}[X(t) + Z(t)] - \mathcal{H}[Z(t)])\end{aligned}\quad (19)$$

is achievable by using the ensemble $X(t)$.⁴ Using the vector version of the entropy power inequality (EPI) [23]

$$e^{\frac{2}{N}h(\mathbf{X}+\mathbf{Y})} \geq e^{\frac{2}{N}h(\mathbf{X})} + e^{\frac{2}{N}h(\mathbf{Y})}, \quad (20)$$

the information rate given by (19) can be lower bounded as

$$\begin{aligned}\mathcal{R} &\geq W \log \left(1 + e^{2\mathcal{H}[X(t)] - 2\mathcal{H}[Z(t)]} \right) \\ &= W \log \left(1 + \frac{\exp(2\mathcal{H}[X(t)])}{2\pi e N_0 W} \right).\end{aligned}\quad (21)$$

Since X_i is i.i.d., the ensemble $X_{\text{PAM}}(t)$ is cyclostationary and the information rate (21) (replacing $X(t)$ with $X_{\text{PAM}}(t)$) is achievable. Now we evaluate $\mathcal{H}[X_{\text{PAM}}(t)]$. We note that the ensemble $X_{\text{PAM}}(t)$ as (17) can be obtained by filtering an ideal bandlimited ergodic ensemble $X_{\text{sync}}(t) = \sum_i X_i g_{\text{sync}}(t - i/2W)$ by $2W \cdot G(f)$. This is because if $g_{\text{sync}}(t)$ is filtered by $2W \cdot G(f)$, the output is $g(t)$ ($G_{\text{sync}}(f) \cdot 2W \cdot G(f) = G(f)$ as $G_{\text{sync}}(f)$ equals $1/2W$ within \mathcal{W}). Then by using Lemma 1 and noting that $\mathcal{H}[X_{\text{sync}}(t)] = h(X)$ (we omit the index of $\{X_i\}$ since they are i.i.d.), we have $\mathcal{H}[X_{\text{PAM}}(t)] = h(X) + \frac{1}{2} \log \mathcal{G}$. Combining this with (21) completes the proof. ■

Theorem 1: The capacity of the AP-BLOIC is lower bounded by

$$\mathcal{C}_{\text{BLOIC}}^{\text{AP}} \geq W \log \left(1 + \frac{\exp(2h(X))}{2\pi e^3 N_0 W} \right) \quad (22)$$

for any $p_X(x)$ satisfying $\mathbb{E}[X] = \mathcal{E}$ and $p_X(x) = 0$ for $x < 0$.

Proof: The proof is given in Appendix A. ■

Theorem 1 is obtained by employing the pulse $g_{\Delta}(t)$ and nonnegative input symbols X_i in (17) and lower bounding the information rate achieved. The maxentropic distribution of a nonnegative random variable with a given expected value \mathcal{E} is the exponential distribution [23]:

$$p_X(x) = \mathcal{E}^{-1} e^{-x/\mathcal{E}}, \quad (23)$$

whose differential entropy is

$$h(X) = \log e\mathcal{E}. \quad (24)$$

Substituting (24) into (22) yields the following corollary.

Corollary 1:

$$\mathcal{C}_{\text{BLOIC}}^{\text{AP}} \geq W \log \left(1 + \frac{1}{2\pi e} \frac{\mathcal{E}^2}{N_0 W} \right). \quad (25)$$

We call (25) the Exp-S2 lower bound since it is based on an input ensemble using exponential symbol distribution and S2

⁴Note that information measures of waveforms, \mathcal{H} and \mathcal{I} , have the same properties as the differential entropy $h(\cdot)$ and mutual information $I(X; Y)$ of scalar variables, respectively, if the limits in (6) and (8) exist.

pulse. While (25) is the tightest bound we could obtain from Theorem 1, the general bound (22) still has its own merit since it can be used to evaluate the performance of more practical input symbol distributions (e.g., a uniform distribution).

Theorem 2: The capacity of the PP-BLOIC is lower bounded by

$$\mathcal{C}_{\text{BLOIC}}^{\text{PP}} \geq W \log \left(1 + \frac{\mathcal{G}}{2\pi e \mathcal{S}_N^2} \frac{\mathcal{A}^2}{N_0 W} \right) \quad (26)$$

where \mathcal{G} and \mathcal{S}_N are defined as (13) and (15), respectively, with respect to an arbitrary modulation pulse $g(t)$ satisfying (10).

Proof: The proof is given in Appendix B. ■

Theorem 2 is derived using an uniform input symbol distribution which is the maxentropic distribution for bounded random variables without further constraint. If we employ $g_{\text{cos}}(t)$ as the modulation pulse and note that for $g_{\text{cos}}(t)$ we have $\mathcal{S}_N = 4/\pi$ and $\mathcal{G} = 1/4$ (see [20]), we get the following corollary called the Unif-cos lower bound which is a suboptimal example of (26).

Corollary 2:

$$\mathcal{C}_{\text{BLOIC}}^{\text{PP}} \geq W \log \left(1 + \frac{\pi}{128e} \frac{\mathcal{A}^2}{N_0 W} \right). \quad (27)$$

Theorem 2 and Corollary 2 can be viewed as parallel results of [20] (in which $g_{\text{cos}}(t)$ is proposed) on lowpass PP-BLAWGN channel.

Theorem 3: The capacity of the PAPR-BLOIC is lower bounded by

$$\mathcal{C}_{\text{BLOIC}}^{\text{PAPR}}(r) \geq \begin{cases} W \log \left(1 + \frac{\mathcal{G} r^2 \exp\left(\frac{2\mathcal{S}_N - r\mathcal{S}_N + r}{r} \mu\right)}{2\pi e \mathcal{S}_N^2} \left(\frac{1 - e^{-\mu}}{\mu}\right)^2 \frac{\mathcal{E}^2}{N_0 W} \right), & r > 2 \\ W \log \left(1 + \frac{\mathcal{G} r^2}{2\pi e \mathcal{S}_N^2} \frac{\mathcal{E}^2}{N_0 W} \right), & 0 < r \leq 2, \end{cases} \quad (28)$$

where r is the PAPR, \mathcal{G} and \mathcal{S}_N are defined as (13) and (15), respectively, with respect to an arbitrary modulation pulse $g(t)$ satisfying (10), and μ is the unique solution to

$$\frac{2\mathcal{S}_N - r\mathcal{S}_N + r}{2r} = \frac{1}{\mu} - \frac{e^{-\mu}}{1 - e^{-\mu}}, \quad (29)$$

Proof: The proof is given in Appendix C. ■

In the proof of Theorem 3, we let the input symbol distribution be a truncated exponential distribution which is the maxentropic distribution of a nonnegative random variable with a given expected value and an upper bound. This distribution was used for bounding the capacity of the DTIOC in [4]. See Appendix C for details.

Note: For the PAPR-DTOIC, when $r \leq 2$ the AP constraint becomes inactive and the capacity is equal to that of the PP-DTOIC with the same PP constraint [4]. For the PAPR-BLOIC, however, it is nontrivial to find out the PAPR transition point at which the AP constraint becomes inactive. Note that $r = 2$ is only the transition point in (28), which is not the capacity.

By employing the pulse $g_{\Delta}(t)$ in (28) we get the following specific lower bound, called the TE-S2 (truncated-exponential-S2) lower bound, which is a suboptimal example of (28).

Corollary 3:

$$C_{\text{BLOIC}}^{\text{PAPR}}(r) \geq \begin{cases} W \log \left(1 + \frac{r^2 e^{2\mu/r}}{2\pi e^3} \left(\frac{1-e^{-\mu}}{\mu} \right)^2 \frac{\mathcal{E}^2}{N_0 W} \right), & r > 2 \\ W \log \left(1 + \frac{r^2}{2\pi e^3} \frac{\mathcal{E}^2}{N_0 W} \right), & 0 < r \leq 2, \end{cases} \quad (30)$$

where $r > 2$, and μ is the unique solution to

$$\frac{1}{r} = \frac{1}{\mu} - \frac{e^{-\mu}}{1 - e^{-\mu}}. \quad (31)$$

Proof: The proof is given in Appendix C. ■

C. ISI-Free Signaling based Capacity Lower Bounds

The results in this subsection are given in the form of lower bounds on $\mathcal{R}_{\text{BLOIC}}^{\text{PC, IFS}}$, which is the maximum achievable information rate of ISI-free signaling over the PC-BLOIC. Of course, they are also lower bounds on the capacity of the PC-BLOIC.

ISI-free signaling avoids ISI by using modulation pulses that satisfy the Nyquist criterion [15]. It may use Nyquist pulses (e.g., raised-cosine pulse) and a direct-sampling detector, or alternatively use the so-called T -orthogonal pulses (e.g., root raised-cosine pulse) and a matched filter detector. ISI-free signaling achieves the Nyquist rate only when the sinc pulse is used.

For the BLOIC, [12] recognizes two important facts on ISI-free signaling using *nonnegative* pulses:

- 1) ISI-free signaling is impossible when a matched filter receiver is used.
- 2) ISI-free signaling is possible when a direct-sampling receiver is used. The maximum symbol rate is a half of the Nyquist rate, achieved by employing the pulse $g_{\Delta}(t)$.

The derivations of all the bounds in the following two theorems use the second fact, i.e., employing i.i.d. PAM signaling as (9) with modulation pulse $g_{\Delta}(t)$ and letting $T_s = T_0 = \frac{1}{W}$.

Theorem 4: The maximum achievable information rates of ISI-free signaling over the AP-BLOIC, the PP-BLOIC, and the PAPR-BLOIC, are lower bounded by (32), (33), and (34), respectively:

$$\mathcal{R}_{\text{BLOIC}}^{\text{AP, IFS}} \geq \frac{W}{2} \log \left(1 + \frac{e}{2\pi} \frac{\mathcal{E}^2}{N_0 W} \right); \quad (32)$$

$$\mathcal{R}_{\text{BLOIC}}^{\text{PP, IFS}} \geq \frac{W}{2} \log \left(1 + \frac{1}{2\pi e} \frac{\mathcal{A}^2}{N_0 W} \right); \quad (33)$$

$$\mathcal{R}_{\text{BLOIC}}^{\text{PAPR, IFS}} \geq \begin{cases} \frac{W}{2} \log \left(1 + \frac{r^2 e^{2\mu/r}}{2\pi e} \left(\frac{1-e^{-\mu}}{\mu} \right)^2 \frac{\mathcal{E}^2}{N_0 W} \right), & r > 2 \\ \frac{W}{2} \log \left(1 + \frac{r^2}{2\pi e} \frac{\mathcal{E}^2}{N_0 W} \right), & 0 < r \leq 2, \end{cases} \quad (34)$$

where r is the PAPR, μ is the unique solution to (31).

Proof: The proof is given in Appendix D. ■

Similar to the DOF-optimal bounds, the derivation of the bounds in Theorem 4 uses the maxentropic input symbol distributions for each type of constraint. We call (32), (33), and (34) the Exp-S2-IFS lower bound, the Unif-S2-IFS lower bound,

and the TE-S2-IFS lower bound, respectively. The following result (called the Geom-S2-IFS lower bound), however, uses a geometry distribution which has been proposed in [6] for bounding the capacity of the DTOIC.

Theorem 5:

$$\mathcal{R}_{\text{BLOIC}}^{\text{AP, IFS}} \geq W \cdot \max_l I(\mathbf{Q}_g(l), \mathbf{V}) \quad (35)$$

where $\mathbf{Q}_g(l)$ is a geometric distribution with PDF

$$p_X(x, l) = \sum_{i=0}^{\infty} \frac{l}{l + \mathcal{E}} \left(\frac{\mathcal{E}}{l + \mathcal{E}} \right)^i \delta(x - il), \quad l > 0, \quad (36)$$

and \mathbf{V} is the transition probability of the channel $Y = X + Z$, where $Z \sim \mathcal{N}(0, N_0 W)$.

Proof: The proof is given in Appendix E. ■

The following result is based on DC-aided ISI-free signaling over the BLOIC [13] whose symbol rate can surpass a half of, and even approach, the Nyquist rate.

Theorem 6: The maximum achievable information rates of ISI-free signaling over the AP-BLOIC, PP-BLOIC, and PAPR-BLOIC are lower bounded by (37) (38), and (39), respectively:

$$\mathcal{R}_{\text{BLOIC}}^{\text{AP, IFS}} \geq \sup_{\beta \in (0,1]} \frac{W}{1+\beta} \log \left(1 + \frac{2}{\mathcal{S}_{\beta}^2 \pi e} \frac{\mathcal{E}^2}{N_0 W} \right); \quad (37)$$

$$\mathcal{R}_{\text{BLOIC}}^{\text{PP, IFS}} \geq \sup_{\beta \in (0,1]} \frac{W}{1+\beta} \log \left(1 + \frac{1}{2\mathcal{S}_{\beta}^2 \pi e} \frac{\mathcal{A}^2}{N_0 W} \right); \quad (38)$$

$$\mathcal{R}_{\text{BLOIC}}^{\text{PAPR, IFS}} \geq \begin{cases} \sup_{\beta \in (0,1]} \frac{W}{1+\beta} \log \left(1 + \frac{r^2 \exp\left(\frac{2\mathcal{S}_{\beta} - r\mathcal{S}_{\beta} + r}{r} \mu\right)}{2\mathcal{S}_{\beta}^2 \pi e} \left(\frac{1-e^{-\mu}}{\mu} \right) \frac{\mathcal{E}^2}{N_0 W} \right), & r > 2 \\ \sup_{\beta \in (0,1]} \frac{W}{1+\beta} \log \left(1 + \frac{r^2}{2\mathcal{S}_{\beta}^2 \pi e} \frac{\mathcal{E}^2}{N_0 W} \right), & 0 < r \leq 2, \end{cases} \quad (39)$$

where the parameter \mathcal{S}_{β} , defined as (15), is determined by the normalized Nyquist pulse $g_{\beta}(t)$ used, and μ is the unique solution to

$$\frac{2\mathcal{S}_{\beta} - r\mathcal{S}_{\beta} + r}{2r} = \frac{1}{\mu} - \frac{e^{-\mu}}{1 - e^{-\mu}}. \quad (40)$$

Proof: The proof is given in Appendix F. ■

By using PL pulse as $g_{\beta}(t)$ in Theorem 6, numerical lower bounds are given in Sec. III. The bounds obtained from (37) and (38) are called the Unif-PL-IFS lower bounds and the bound obtained from (39) is called the TE-PL-IFS lower bound. The reason for choosing the PL pulse is as follows. In bias-aided ISI-free signaling over the BLOIC, there is a tradeoff between the required DC bias and the achieved symbol rate: a higher symbol rate requires a larger DC bias (and a larger power cost). This leads to a tradeoff between power and DOF, see Fig. 5 in Sec. III. When the rate of ISI-free signaling is close to the Nyquist rate, the required DC bias increases sharply (cf. Fig. 4 of [13]). Achieving ISI-free signaling at exactly the Nyquist rate is impossible because it requires an infinitely large DC bias. A general analysis on the optimal DC bias-symbol rate tradeoff of arbitrary Nyquist pulses is difficult. But for certain kind of parametric pulses (e.g., raised cosine pulse with a roll off factor β) this tradeoff

TABLE IV
UPPER BOUNDS AND RELATED DTOIC RESULTS

Upper bounds	Related DTOIC result
SP UB3, Fig. 2	[6, (11)]
Dual UB, Fig. 2	[4, (28)]
SP UB1 and SP UB2, Fig. 6	[7, Theorem 1]
Dual UB1, Fig. 6	[4, (19)]
Dual UB2, Fig. 6	[4, (20)]
Dual UB1, Fig. 7	[4, (11)]
Dual UB2, Fig. 7	[4, (12)]

has been numerically characterized in [13] in which the PL pulse was shown to be a good choice in a variety of pulses.

D. Capacity Upper Bounds

The following lemma holds for all the input power constraints given in Table II.

Lemma 3: The capacity of the PC-BLOIC with bandwidth W is upper bounded by

$$C_{\text{BLOIC}}^{\text{PC}} \leq C_{\text{DTOIC}}^{\text{PC}, \sigma^2 = N_0 W} \cdot 2W \text{ transmissions per second} \quad (41)$$

where $C_{\text{DTOIC}}^{\text{PC}}$ is the capacity of the DTOIC under the same type of constraint with equal parameters as the PC-BLOIC.

Proof: The proof is given in Appendix G. ■

Combining Lemma 3 and known capacity upper bounds for the AP-DTOIC, the following capacity upper bounds for the AP-BLOIC are obtained.

Theorem 7: The capacity of the AP-BLOIC is upper bounded by the following two bounds simultaneously:

$$C_{\text{BLOIC}}^{\text{AP}} \leq W \log \left(\frac{e}{2\pi} \left(\frac{\mathcal{E}}{\sqrt{N_0 W}} + 2 \right)^2 \right), \quad (42)$$

$$C_{\text{BLOIC}}^{\text{AP}} \leq \sup_{\alpha \in [0,1]} W \left(\log \left(\frac{e}{2\pi} \frac{\mathcal{E}^2}{N_0 W} \right)^\alpha - \log(1 - \alpha)^{2-2\alpha} \alpha^{3\alpha} \right). \quad (43)$$

Proof: By Lemma 3 and the upper bounds for the AP-DTOIC from [3, eqn. (21)] (implicitly given therein) and [7, eqn. (1)], (42) and (43) are obtained, respectively. ■

Remark 1: More capacity upper bounds for the AP-BLOIC can be obtained by other capacity upper bounds for the AP-DTOIC. Parallel results of Theorem 7 for the PP- and PAPR-BLOIC can be similarly obtained. Since the mathematical expressions of these results can be written out directly based on the corresponding DTOIC results, we only give them numerically in Sec. III, and list them in Table IV. According to the type of the related DTOIC results, we categorize these upper bounds as sphere-packing based ones (SP UB) and duality based ones (Dual UB).

III. COMPARISONS OF BOUNDS

In this section we give numerical evaluation of our results. In all figures the SNR and PNR of the BLOIC is defined as $\text{SNR} = \frac{\mathcal{E}}{\sqrt{N_0 W}}$ and $\text{PNR} = \frac{A}{\sqrt{N_0 W}}$, respectively.

In Fig. 2 our main results on the AP-BLOIC are plotted. At high SNR, it is shown that the Exp-S2 lower bound (25) and the upper bound (42) are the tightest lower and upper bounds, respectively. Moreover, they have the same asymptotic slope and the high SNR asymptotic gap between them is 4.34 dB in SNR or 2.89 bit/s/Hz in spectral efficiency.

For comparison, the information rate bounds in [3] for a specific TDS scheme called 3-PSWF, whose lower bound is the best among all examples in [3], are also plotted in Fig. 2. It is clear that the lower bound increases very slowly with SNR and the upper bound is not a capacity upper bound for the AP-BLOIC.⁵ Moreover, a high SNR asymptotic upper bound for the AP-BLOIC based on the result of [11] is also shown and the details about this bound are given in Sec. IV.

An important observation is that ISI-free signaling performs well for all practical SNR values (e.g. in Fig. 2 we show the SNR range $[-8, 22]$ in dB). At low to moderate SNR, all the ISI-free signaling based lower bounds outperform the Exp-S2 lower bound (25), and the Geom-S2-IFS lower bound (35) is the tightest one. At high SNR, the Unif-PL-IFS lower bound (37) obtained by DC bias aided ISI-free signaling achieves information rates close to the best known capacity lower bound obtained without ISI-free constraint.

Fig. 3 and Fig. 4 show the AP-BLOIC capacity lower bounds in the low to moderate SNR regime. The information rates of regular PAM constellations based (TDS) schemes of [3] are also given for comparison. Only when the SNR is below 0 dB, the TDS schemes may have similar information rates compared with some of our lower bounds. The lower bound (35) stands out from all the results at low to moderate SNR.

Fig. 5 shows the information rates of DC bias aided ISI-free signaling using $g_{\text{PL}}(t)$ under different roll-off factors (i.e. the RHS of (37) excluding the supremum operation), and a tradeoff between low-SNR and high-SNR information rates for a given β is clear. As practical systems always use a fixed β , a carefully chosen β (typically from 0.15 to 0.4) may balance the performance for most practical SNR values.

Fig. 6 and Fig. 7 show the capacity bounds for the PP- and PAPR-BLOIC (where $r = 2.5$), respectively. The behavior of these bounds are similar to that in the AP-BLOIC case. Note that at low SNR (33) and (34) are equal to (38) and (39), respectively.

In Fig. 8 we show the lower bounds on the capacity of the PAPR-BLOIC given by (30) for different PAPR values, where all the bounds are derived using the S2 pulse. Meanwhile, (25) is given as a benchmark since it can be viewed as the case of $r = \infty$, noting that as $r \rightarrow \infty$, μ tends to r , and the RHS of (30) monotonically increases and tends to the RHS of (25). For

⁵A 0.99-fractional bandwidth definition is used in the evaluation of the performance of 3-PSWF (also the TDS based PAM results in Fig. 3 and Fig. 4). Although the PSWF who achieve the best time-frequency concentration are used, the total DOF efficiency is dominated by the rectangular basis function which always exists in TDS signal space models.

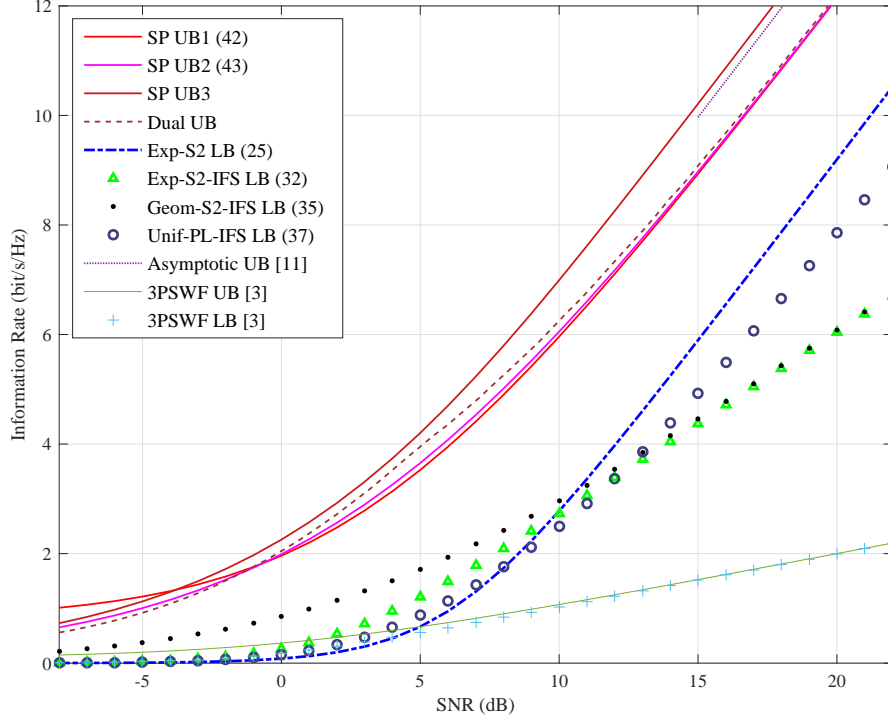


Fig. 2. Upper bounds (UB) and lower bounds (LB) for the capacity of the AP-BLOIC.

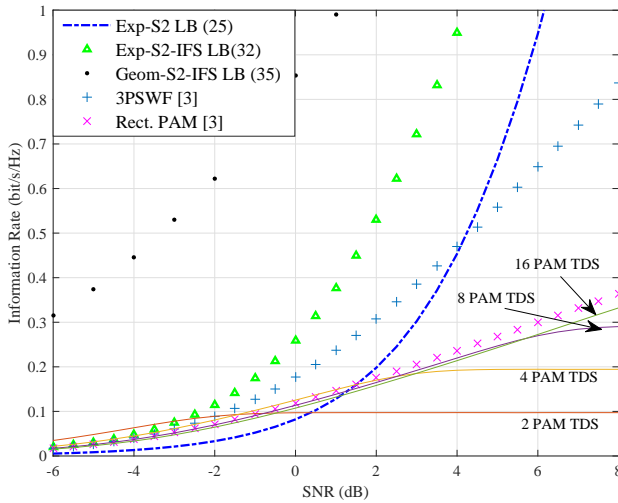


Fig. 3. Lower bounds on $C_{\text{BLOIC}}^{\text{AP}}$: moderate SNR region.

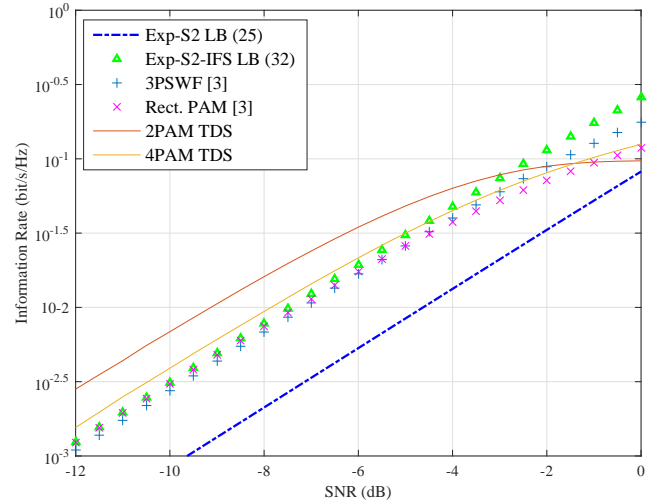


Fig. 4. Lower bounds on $C_{\text{BLOIC}}^{\text{AP}}$: low SNR region.

our bounds, it is shown that the PAPR constraint only causes some SNR loss. Moreover, an example of the capacity lower bound of the BLOIC with input constraint $\mathcal{P}_{\{X\}} \leq \mathcal{E}$, $0 \leq x(t) \leq \mathcal{A}_0$ (called AP-PP-BLOIC, where \mathcal{A}_0 is a constant) is given, denoted as AP-PP LB. It is obtained by setting PAPR $r = \mathcal{A}_0/\mathcal{E}$ in Corollary 3 for each SNR. The value of \mathcal{A}_0 is set to be 10 dB higher than the noise variance. When the SNR is relatively low, the PAPR is large so that the bound is close

to the Exp-S2 LB. When the SNR exceeds 7 dB the bound stops increasing.

IV. DISCUSSIONS AND CONJECTURES

This section discusses further improvement of our lower and upper bounds, since there are still considerable gaps between them. We believe that new bounding techniques are needed

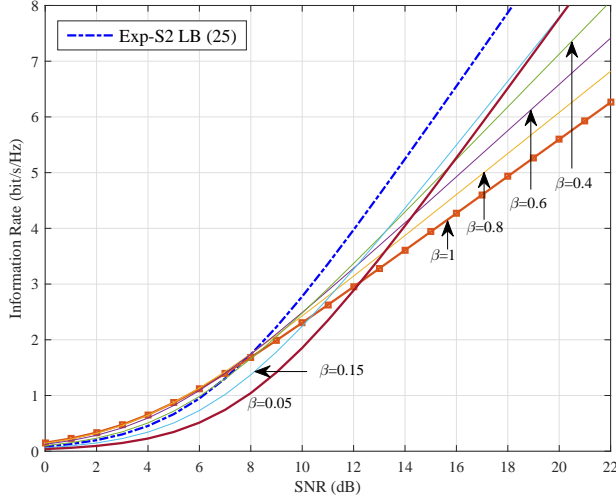


Fig. 5. Information rates of DC bias aided ISI-free signaling using $g_{PL}(t)$ under different roll-off factors.

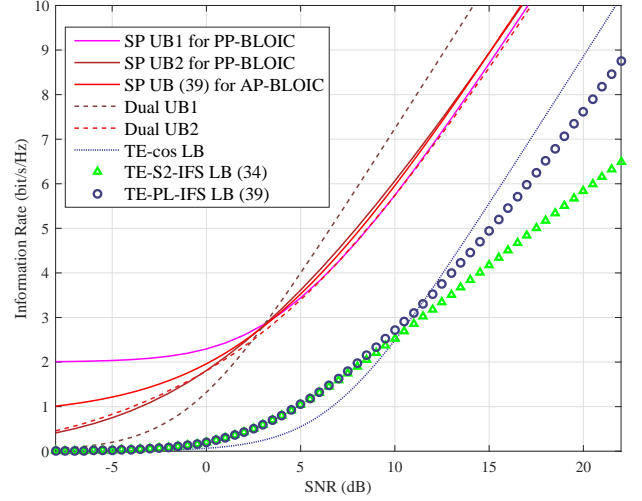


Fig. 7. Upper and lower bounds on the capacity of the PAPR-BLOIC, $r = 2.5$.

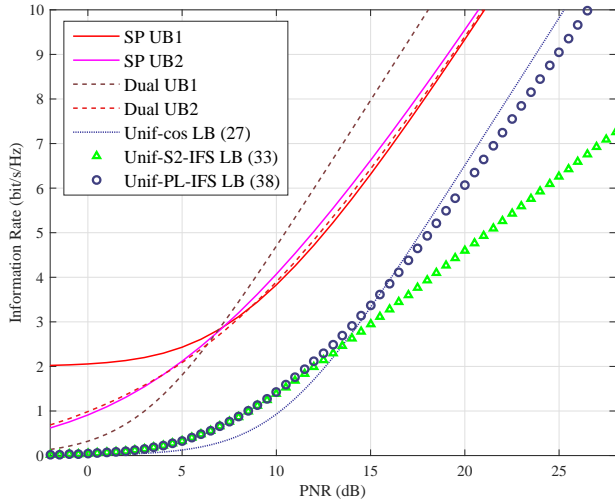


Fig. 6. Upper and lower bounds on the capacity of the PP-BLOIC.

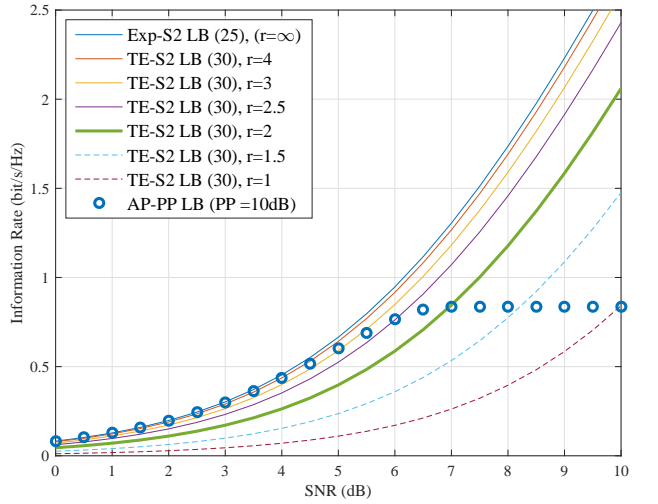


Fig. 8. Lower bounds on the capacity of the PAPR-BLOIC and the AP-PP-BLOIC.

to tighten the gap. We give two conjectures which considers lower and upper bounding, respectively.

Our DOF-optimal capacity lower bounds have a general form of

$$\mathcal{C}_{\text{BLOIC}}^{\text{PC}} \geq W \log \left(1 + \eta \frac{\mathcal{E}^2}{N_0 W} \right). \quad (44)$$

In Theorem 2 and Theorem 3, η can be maximized by finding out the optimal $g(t)$ that maximizes $\mathcal{G}/\mathcal{S}_N^2$. However, this is still an open problem. Moreover, the optimal $g(t)$ for the PAPR-BLOIC may vary for different PAPR values. In Fig. 9, the values of η in the lower bounds on the capacity of the PAPR-BLOIC obtained by using $g_{\Delta}(t)$ and $g_{\cos}(t)$ in Theorem 3 are given for different PAPR values. It is shown that when r is smaller than 2.7, $g_{\cos}(t)$ is better, and otherwise $g_{\Delta}(t)$ is better. For large PAPR values, finding out a pulse which achieves larger η than that obtained by $g_{\Delta}(t)$ is difficult,

because a $G(f)$ with relatively large \mathcal{G} always has large sidelobes in the time domain, which also causes large \mathcal{S} . Due to the time-frequency uncertainty, we cannot make $\mathcal{G}/\mathcal{S}_N^2$ very large. In summary, we have the following conjecture:

Conjecture 1: The high-SNR asymptotic capacity expression of i.i.d. Nyquist rate PAM signaling over the AP-BLOIC, denoted as $\mathcal{C}_{\text{BLOIC}}^{\text{AP, i.i.d. NRP}}$, satisfies

$$\lim_{\text{SNR} \rightarrow \infty} \left\{ \mathcal{C}_{\text{BLOIC}}^{\text{AP, i.i.d. NRP}} - W \log \left(1 + \frac{1}{2\pi e} \frac{\mathcal{E}^2}{N_0 W} \right) \right\} = 0. \quad (45)$$

For the capacity of the AP-DTOIC, the high-SNR asymptotically tight bounds reported in [3] (implicitly) and in [4], [6] imply that

$$\lim_{\text{SNR} \rightarrow \infty} \left\{ \mathcal{C}_{\text{DTOIC}}^{\text{AP}} - \log \frac{\lambda \mathcal{E}}{\sigma} \right\} = 0 \quad (46)$$

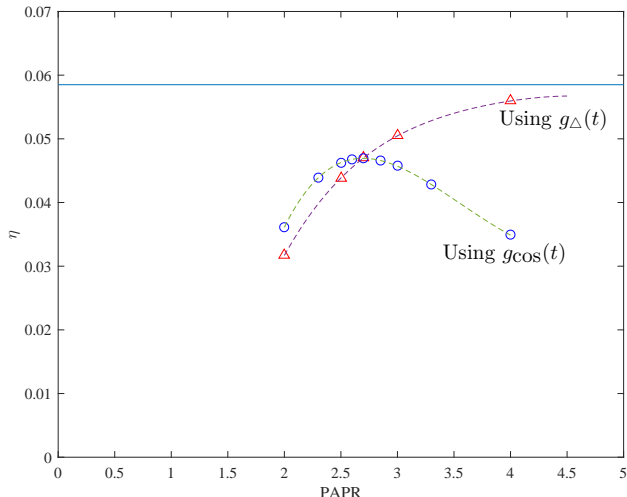


Fig. 9. Behavior of η for two specific modulation pulses in the PAPR-BLOIC.

where $\lambda = \sqrt{\frac{e}{2\pi}}$. Our tightest capacity bounds for the AP-BLOIC at high SNR, (25) and (42), have the same pre-log factor but different pre-SNR factors:

$$2W \log \left(\lambda \frac{\mathcal{E}}{\sqrt{N_0 W}} + 2\lambda \right) \geq C_{\text{BLOIC}}^{\text{AP}} \geq 2W \log \frac{\lambda}{e} \frac{\mathcal{E}}{\sqrt{N_0 W}}. \quad (47)$$

We may thus expect that

$$\lim_{\text{SNR} \rightarrow \infty} \left\{ C_{\text{BLOIC}}^{\text{AP}} - 2W \log \frac{\rho \lambda \mathcal{E}}{\sqrt{N_0 W}} \right\} = 0. \quad (48)$$

where $\rho \leq 1$ is a factor determining the high SNR capacity of the AP-BLOIC. The existence and value of the factor ρ in (48) is of interest to us because if ρ is strictly less than one, then we can conclude that when we simplify the BLOIC to a DTOIC which transmits $2W$ times per second, there does exist a penalty on capacity because of the fundamental distinction between the BLOIC and the DTOIC. We have the following conjecture.

Conjecture 2: The factor ρ in (48) exists and satisfies $\rho < 1$.

Remark 2: A possible way of settling Conjecture 2 is using the sphere packing based upper bounding technique in [11], by which we can get a high-SNR asymptotic upper bound on the capacity of the AP-BLOIC as

$$\lim_{\text{SNR} \rightarrow \infty} \left\{ C_{\text{BLOIC}}^{\text{AP}} - W \log \left(\lim_{K \rightarrow \infty} K (\text{Vol}(\Upsilon^K))^{\frac{1}{K}} \frac{2}{\pi e} \frac{\mathcal{E}^2}{N_0 W} \right) \right\} \leq 0, \quad (49)$$

where Υ^K is the admissible region of length- K input symbol sequences as

$$\Upsilon^K = \left\{ [c_k]_{k=1}^K : \frac{1}{2} + \text{Re} \left[\sum_{k=1}^K c_k \exp \frac{-j2k\pi W t}{K} \right] \geq 0, c_k \in \mathbb{C} \right\}, \quad (50)$$

and $\text{Vol}(\Upsilon^K)$ is its volume. Conjecture 2 can be proved if we can show that $\lim_{K \rightarrow \infty} K (\text{Vol}(\Upsilon^K))^{\frac{1}{K}} < e^2/4$. However, a direct calculation of this limit or even its upper bound is nontrivial. In [11] it was proved that Υ^K is a subset of a K -dimensional trigonometric moment space \mathcal{M}^K whose volume has been determined to satisfy $\lim_{K \rightarrow \infty} K (\text{Vol}(\mathcal{M}^K))^{\frac{1}{K}} < \pi e/2$. Thus we have the asymptotic upper bound shown in Fig. 2, based on (49). Unfortunately this is not enough for settling Conjecture 2.

Note: In fact, Υ^K is the admissible region of the input of the AP-MCOIC with K subcarriers and a nominal bandwidth W . As $K \rightarrow \infty$, [11] shows that the high-SNR asymptotic capacity of the AP-MCOIC is upper bounded by $W \log \frac{\mathcal{E}^2}{N_0 W}$.⁶ We note that each asymptotic result obtained by (49) is also a high-SNR asymptotic upper bound on the capacity of the AP-BLOIC, although it is obtained from considering the AP-MCOIC. The interpretation is as follows. For a fixed W , K tending to infinity is equivalent to the length of a $\frac{1}{2W}$ -interval sample sequence of a block of input of the MCOIC tending to infinity. Meanwhile, the out-of-band energy of the MCOIC in the sense of nominal bandwidth decreases to zero, and the time domain $\frac{1}{2W}$ -interval samples of the MCOIC reduce to the Nyquist samples. In summary, as K tends to infinity, the limit of the admissible region of the input of the AP-MCOIC tends to the admissible region of the input of the AP-BLOIC with bandwidth W . So the capacity of the AP-MCOIC converges to the capacity of the AP-BLOIC whose bandwidth is equal to W .

APPENDIX A

Consider an i.i.d. Nyquist rate PAM ensemble using $g_\Delta(t)$ as

$$\begin{aligned} X_\Delta(t) &= \sum_i X_i g_\Delta \left(t - \frac{i}{2W} \right) \\ &= \sum_i X_i \frac{\sin^2 \pi W (t - i/2W)}{2(\pi W (t - i/2W))^2}. \end{aligned} \quad (51)$$

Let the input symbols be i.i.d. nonnegative (which guarantees the nonnegativity of $X_\Delta(t)$ since $g_\Delta(t)$ is nonnegative) and let $\text{E}[X]$ be equal to \mathcal{E} . Then the AP of $X_\Delta(t)$ is

$$\begin{aligned} \mathcal{P}_{\{X_\Delta\}} &= \lim_{T \rightarrow \infty} \frac{1}{2T} \text{E} \left[\int_{-T}^T \sum_{i=-\infty}^{\infty} X_i \frac{\sin^2 \pi W (t - iT_s)}{2(\pi W (t - iT_s))^2} dt \right] \\ &= \lim_{N \rightarrow \infty} \frac{1}{2NT_s} \int_{-NT_s}^{NT_s} \sum_{i=-\infty}^{\infty} \text{E}[X_i] \frac{\sin^2 \pi W (t - iT_s)}{2(\pi W (t - iT_s))^2} dt \\ &= \mathcal{E} \cdot \lim_{N \rightarrow \infty} \frac{1}{2NT_s} \sum_{n=-N}^{N-1} \int_{nT_s}^{(n+1)T_s} \sum_{i=-\infty}^{\infty} \frac{\sin^2 \pi W (t - iT_s)}{2(\pi W (t - iT_s))^2} dt \\ &= \mathcal{E} \cdot \lim_{N \rightarrow \infty} \frac{1}{2NT_s} \sum_{n=-N}^{N-1} \sum_{i=-\infty}^{\infty} \int_{nT_s}^{(n+1)T_s} \frac{\sin^2 \pi W (t - iT_s)}{2(\pi W (t - iT_s))^2} dt \end{aligned}$$

⁶The expression of this result is different from [11, (56)] (when the channel gain is normalized to one) because [11] used a nonstandard definition of the power spectral density of the white Gaussian noise.

$$\begin{aligned}
&= \mathcal{E} \cdot \lim_{N \rightarrow \infty} \frac{1}{2NT_s} \sum_{n=-N}^{N-1} \sum_{i=-\infty}^{\infty} \int_{(n-i)T_s}^{(n+1-i)T_s} \frac{\sin^2 \pi W t'}{2(\pi W t')^2} dt' \\
&= \mathcal{E} \cdot \lim_{N \rightarrow \infty} \frac{1}{2NT_s} 2N \int_{-\infty}^{\infty} \frac{\sin^2 \pi W t}{2(\pi W t)^2} dt \\
&= \mathcal{E} \cdot \frac{1}{T_s} \cdot \frac{1}{2W} \\
&= \mathcal{E}, \tag{52}
\end{aligned}$$

where the second equality follows by the linearity of expectation and letting $T = NT_s$, the third by dividing the interval of integration, the fourth by noting that the infinite sum converges for $t \in \mathbb{R}$, the fifth by defining $t' \triangleq t - iT_s$, and the sixth by noting that the integrals over all the intervals $[(n-i)T_s, (n+1-i)T_s]$ sum to the integral over $(-\infty, \infty)$. Thus the AP constraint is satisfied, and $X_{\Delta}(t)$ is admissible for the AP-BLOIC. Since

$$G_{\Delta}(f) = \begin{cases} \frac{1}{2W} \frac{W-|f|}{W}, & |f| \leq W \\ 0, & \text{otherwise,} \end{cases} \tag{53}$$

we have

$$\begin{aligned}
\mathcal{G} &= \exp \left(\frac{1}{W} \int_0^W \log |2W \cdot G_{\Delta}(f)|^2 df \right) \\
&= \exp \left(\frac{2}{W} \int_0^W \log \left(\frac{W-f}{W} \right) df \right) \\
&= \frac{1}{e^2}. \tag{54}
\end{aligned}$$

Substituting (54) into (18) completes the proof of Theorem 1.

APPENDIX B

Consider the i.i.d. Nyquist rate PAM ensemble $X_{\text{PAM}}(t)$ as (17). By letting X_i be bounded within $[-\frac{\mathcal{A}}{2S_N}, \frac{\mathcal{A}}{2S_N}]$, we can make the ensemble satisfy $-\frac{\mathcal{A}}{2} \leq X_{\text{PAM}}(t) \leq \frac{\mathcal{A}}{2}$, according to the definition of S_N . Let a DC bias $\mathcal{D} = \mathcal{A}/2$ be added to $X_{\text{PAM}}(t)$, and thus the nonnegativity and PP constraints of the PP-BLOIC are both satisfied. The maximum differential entropy of X_i is $h(X) = \log \frac{\mathcal{A}}{S_N}$ and is obtained by letting X_i be uniformly distributed. Using Lemma 2, (26) is obtained immediately.

APPENDIX C

For the case of $r > 2$, let us consider the i.i.d. Nyquist rate PAM ensemble $X_{\text{PAM}}(t)$ as (17). Assume the inputs X_i to be bounded within $[0, L]$ and let $E[X_i] = L/\nu$, $\nu \geq 2$, where ν is the PAPR of X_i . The maxentropic distribution of X_i is a truncated exponential distribution according to [4, eqn. (42)],

$$p_X(x) = \frac{1}{L} \frac{\mu}{1 - e^{-\mu}} e^{-\frac{\mu x}{L}}, \quad 0 \leq x \leq L, \tag{55}$$

where μ is the unique solution of

$$\frac{1}{\nu} = \frac{1}{\mu} - \frac{e^{-\mu}}{1 - e^{-\mu}}. \tag{56}$$

The differential entropy of (55) is

$$h(X) = \frac{\mu}{\nu} + \log \left(L \frac{1 - e^{-\mu}}{\mu} \right). \tag{57}$$

Then the maximum achievable information rate of $X_{\text{PAM}}(t)$ can be lower bounded by

$$\mathcal{R}[X(t)] \geq W \log \left(1 + \frac{\mathcal{G}\nu^2 e^{2\mu/\nu}}{2\pi e} \left(\frac{1 - e^{-\mu}}{\mu} \right)^2 \frac{L^2}{\nu^2 N_0 W} \right), \tag{58}$$

which follows from Lemma 2 by using the distribution (55).

We now design $X_{\text{PAM}}(t)$ to be an admissible input ensemble of the PAPR-BLOIC with PAPR r and convert (58) into a capacity lower bound of the PAPR-BLOIC with parameters r , \mathcal{E} , \mathcal{G} , and S_N . We first shift the distribution of X_i by $-\frac{L}{2}$ so that X_i is distributed in $[-\frac{L}{2}, \frac{L}{2}]$. Now its mean becomes

$$E[X_i] = \frac{L}{\nu} - \frac{L}{2}. \tag{59}$$

The corresponding i.i.d. Nyquist rate PAM ensemble, denoted as $X_0(t)$, satisfies

$$-\frac{S_N L}{2} \leq X_0(t) \leq \frac{S_N L}{2}. \tag{60}$$

By adding a DC bias $\mathcal{D} = \frac{S_N L}{2}$ on $X_0(t)$, we obtain an admissible waveform ensemble $X_{\text{PAM}}(t)$ that satisfies $0 \leq X(t) \leq S_N L$. The PP constraint is satisfied by letting $S_N L$ be equal to $r\mathcal{E}$. Since the mean of $X_0(t)$ is equal to $E[X_i]$, i.e. the mean of the input symbol (cf. the derivation of (52)), the AP of $X_{\text{PAM}}(t)$ is

$$\mathcal{E} = \mathcal{D} + E[X_i] = \frac{2 - \nu + \nu S_N}{2\nu} L. \tag{61}$$

The PAPR of $X_{\text{PAM}}(t)$ is r if we set ν as

$$\nu = \frac{2r}{2S_N - rS_N + r}. \tag{62}$$

According to (62) and $S_N L = r\mathcal{E}$, we can convert (58) into a general capacity lower bound of the PAPR-BLOIC as the case of $r > 2$ in Theorem 3.

For the case of $0 < r \leq 2$, consider the designed input ensemble $X_{\text{PAM}}(t)$ (after DC bias being added) in the proof of Theorem 2 in Appendix B. Apparently the AP of $X_{\text{PAM}}(t)$ is $\mathcal{A}/2$. If we let $\mathcal{A} = r\mathcal{E}$, the AP of $X_{\text{PAM}}(t)$ is then $r\mathcal{E}/2$ which is smaller than \mathcal{E} since $r < 2$. So $X_{\text{PAM}}(t)$ is also admissible for the PAPR-BLOIC with $r < 2$ and $r\mathcal{E} = \mathcal{A}$. Replacing \mathcal{A} in (26) by $r\mathcal{E}$, the case of $0 < r < 2$ is obtained and the proof of Theorem 3 is completed.

Corollary 3 follows immediately from Theorem 3 by letting $g(t)$ be $g_{\Delta}(t)$ and noting that in this case $\mathcal{G} = 1/e^2$ (see (54)) and $S_N = 1$ (this was implicitly shown in [18]).

APPENDIX D

Consider the following input ensemble which achieves ISI-free signaling according to [12]:

$$X_{\Delta}^{\text{IFS}}(t) = \sum_i X_i \frac{\sin^2 \pi W(t - i/W)}{(\pi W(t - i/W))^2}, \tag{63}$$

where the pulse used is a scaling of $g_{\Delta}(t)$ with a factor of two so as to satisfy Definition 1. Letting the input symbols $\{X_i\}$ be i.i.d. and satisfy $E[X] = \mathcal{E}$, then the AP of the input ensemble is $\mathcal{P}_{\{X\}} = \mathcal{E}$ (cf. the derivation of (52), noting that the time domain integral of the pulse used here is $1/W$). Denote

the equivalent discrete-time memoryless channel of ISI-free signaling over the BLOIC using (63), which is obtained from $\frac{1}{W}$ -interval sampling at the receiver, as

$$Y[i] = X[i] + Z[i]. \quad (64)$$

The value of $g(0)$ determines the noiseless sample values when the corresponding input symbols are given. Since $2 \cdot g_{\Delta}(0) = 1$, the noiseless samples satisfy $X[i] \equiv X_i$. The variance of the noise samples can be minimized by an ideal bandlimited filtering over \mathcal{W} on the received noisy waveform, not affecting the value of $X[i]$ in (64) and preserving the memoryless property of noise samples. So the obtained noise samples $Z[i]$ are i.i.d. with variance N_0W . Then if we let X_i be exponentially distributed as (23), we have

$$\begin{aligned} \mathcal{R}[X_{\Delta}^{\text{IFS}}(t)] &= W \cdot I(X[i], Y[i]) \\ &= W \cdot (h(Y[i]) - h(Z[i])) \\ &\geq \frac{W}{2} \log \left(1 + e^{2h(X_i) - 2h(Z[i])} \right) \\ &= \frac{W}{2} \log \left(1 + \frac{e}{2\pi} \frac{\mathcal{E}^2}{N_0W} \right), \end{aligned} \quad (65)$$

where the inequality follows from the EPI, and (32) is obtained.

The proofs of (33), the first case of (34), and the second case of (34) are similar except that we let X_i be uniformly distributed in $[0, \mathcal{A}]$, truncated-exponentially distributed in $[0, r\mathcal{E}]$ (whose PDF can be obtained from (55) by replacing L with $r\mathcal{E}$ and replacing ν with r), and uniformly distributed in $[0, r\mathcal{E}]$, respectively.

APPENDIX E

The proof of Theorem 5 can be done by a variation on the proof of Theorem 4 as follows. Note that (64) can be viewed as a DTOIC where $Z_i \sim \mathcal{N}(0, N_0W)$, transmitting only W times per second. So we have

$$\mathcal{R}_{\text{BLOIC}}^{\text{AP, IFS}} \geq \mathcal{C}_{\text{DTOIC}}^{\text{AP}, \sigma^2=N_0W} \cdot W \text{ transmissions per second.} \quad (66)$$

Now all capacity lower bounds of the AP-DTOIC can be used to derive a lower bound for the maximum achievable information rate of ISI-free signaling over the AP-BLOIC. The tightest known capacity lower bound of the DTOIC is in [6], where a geometric distribution as (36) is used as the input distribution. The parameter l (space between mass points of geometric distribution) in (36) is optimized for each SNR to maximize the information rate achieved by such lower bound. That information rate is thus $\max_l I(\mathbf{Q}_g(l), \mathbf{V})$. The proof of

Theorem 5 is then completed by replacing $\mathcal{C}_{\text{DTOIC}}^{\text{AP}, \sigma^2=N_0W}$ in (66) by $\max_l I(\mathbf{Q}_g(l), \mathbf{V})$.

APPENDIX F

Consider the i.i.d PAM ensemble $X_{\text{PAM}}(t)$ as (9) in which we let $g(t)$ be a Nyquist pulse satisfying Definition 1 and T_s be $\frac{1+\beta}{2W}$ so that the ISI-free property is achieved. Let the input symbols X_i be uniformly distributed in $[-L/2, L/2]$. Since $E[X_i] = 0$, the mean of the ensemble obtained is also zero (cf. the derivation in (52)). According to the definition of $\mathcal{S}(\tau)$,

we have $-\frac{1}{2}\mathcal{S}_{\beta}L \leq X_{\text{PAM}}(t) \leq \frac{1}{2}\mathcal{S}_{\beta}L$. So the DC bias needed is $\frac{1}{2}\mathcal{S}_{\beta}L$, and the mean (AP) of $X_{\text{PAM}}(t)$ becomes

$$\mathcal{E} = \frac{\mathcal{S}_{\beta}L}{2}, \quad (67)$$

with that DC bias.

Consider the equivalent discrete-time channel of such ISI-free signaling, denoted as $Y[i] = X[i] + Z[i]$ (cf. the derivation of (65)). Since $X[i]$ is uniformly distributed, from (67) we have

$$h(X[i]) = \log L = \log \frac{2\mathcal{E}}{\mathcal{S}_{\beta}}. \quad (68)$$

So the maximum achievable information rate can be lower bounded as (cf. (65))

$$\begin{aligned} \mathcal{R} &= \frac{2W}{1+\beta} \cdot I(X[i], Y[i]) \\ &\geq \frac{W}{1+\beta} \log \left(1 + e^{2h(X[i]) - 2h(Z[i])} \right) \\ &= \frac{W}{1+\beta} \log \left(1 + \frac{2}{\mathcal{S}_{\beta}^2 \pi e} \frac{\mathcal{E}^2}{N_0W} \right), \end{aligned} \quad (69)$$

where the inequality follows from the EPI, and (37) is obtained immediately. This completes the proof of (37).

Since the input ensemble obtained in the proof of (37) is bounded in $[0, \mathcal{S}_{\beta}L]$, by letting $L = \frac{\mathcal{A}}{\mathcal{S}_{\beta}}$ the same input ensemble is admissible for the PP-BLOIC. Combining $L = \frac{\mathcal{A}}{\mathcal{S}_{\beta}}$, (67), and (69) we obtain (38).

Consider a truncated exponential distribution \mathbf{Q}_{TE} whose PDF is as (55) except letting

$$\mathcal{S}_{\beta}L = r\mathcal{E}, \quad \nu = \frac{2r}{2\mathcal{S}_{\beta} - r\mathcal{S}_{\beta} + r}. \quad (70)$$

From the proof of Theorem 3, we know that if we use such an input symbol distribution to replace the uniform distribution used in the proof of (37), the obtained input ensemble is admissible for the PAPR-BLOIC (i.e. the AP equals \mathcal{E} and the PAPR equals r) after adding a minimum required DC bias. Replace the $h(X[i])$ in (69) by the differential entropy of \mathbf{Q}_{TE} (which is obtained by combining (70) and (57)) we obtain the first case of (39). For the second case we alternatively use an uniform distribution \mathbf{Q}_{U} in $\left[0, \frac{r\mathcal{E}}{\mathcal{S}_{\beta}}\right]$ which guarantees the obtained input ensemble satisfying the PP constraint. Noting that the AP constraint is also satisfied, the second case of (39) can be obtained from replacing the $h(X[i])$ in (69) by the differential entropy of \mathbf{Q}_{U} . This completes the proof of Theorem 6.

APPENDIX G

Consider a bandlimited channel as $Y(t) = X(t) + Z(t)$ (where $Z(t)$ is defined as in (1)), denoted as channel A, with a relaxed version of input power constraint PC as follows: 1) the nonnegativity and PP constraints on $X(t)$ hold only at $t = n/2W, \forall n \in \mathbb{Z}$, i.e. on a sequence of Nyquist sample points; 2) the AP constraint is defined like that in the BLOIC. Obviously, the capacity of this channel, denoted as $\mathcal{C}_{\text{A}}^{\text{PC-relaxed}}$, is an upper bound of $\mathcal{C}_{\text{BLOIC}}^{\text{PC}}$. Each input ensemble of channel A, denoted as $X_{\text{A}}(t)$, can be viewed as an i.i.d. Nyquist

rate PAM ensemble as (17) where $g(t) = g_{\text{sinc}}(t)$ and the input symbols $\{X_i\}$ are just the Nyquist samples of $X_A(t)$. By matched filtering $X_A(t)$ with $2W \cdot G_{\text{sinc}}(f)$ and sampling at Nyquist intervals (an information lossless procedure), an equivalent model of channel A is obtained as the following discrete-time memoryless channel:

$$Y[i] = X[i] + Z[i], \quad (71)$$

where $X[i] = X_i$, and $Z[i] \sim \mathcal{N}(0, N_0W)$. This channel is a DTOIC with the same type of constraints and corresponding parameters per the constraint PC of channel A. Since this channel transmits $2W$ symbols per second, we have

$$\begin{aligned} \mathcal{C}_{\text{BLOIC}}^{\text{PC}} &\leq \mathcal{C}_A^{\text{PC-relaxed}} \\ &= \mathcal{C}_{\text{DTOIC}}^{\text{PC}, \sigma^2=N_0W} \cdot 2W \text{ transmissions per second.} \end{aligned} \quad (72)$$

This completes the proof of Lemma 3.

ACKNOWLEDGEMENTS

The authors would like to thank the anonymous reviewers for their comments which helped to significantly improve the manuscript.

REFERENCES

- [1] S. Hranilovic, "On the design of bandwidth efficient signalling for indoor wireless optical channels," *Int. J. Commun. Syst.*, vol. 18, no.3, pp. 205–228, 2005.
- [2] M. A. Khalighi and M. Uysal, "Survey on free space optical communication: a communication theory perspective," *IEEE Commun. Surveys Tuts.*, vol. 16, no. 4, pp. 2231–2258, fourth quarter 2014.
- [3] S. Hranilovic and F. R. Kschischang, "Capacity bounds for power- and band-limited optical intensity channels corrupted by Gaussian noise," *IEEE Trans. Inf. Theory*, vol. 50, no. 5, pp. 784–795, May 2004.
- [4] A. Lapidoth, S. M. Moser, and M. A. Wigger, "On the capacity of free-space optical intensity channels," *IEEE Trans. Inf. Theory*, vol. 55, no. 10, pp. 4449–4461, Oct. 2009.
- [5] A. A. Farid and S. Hranilovic, "Channel capacity and non-uniform signalling for free-space optical intensity channels," *IEEE J. Sel. Areas Commun.*, vol. 27, no. 9, pp. 1553–1563, Dec. 2009.
- [6] A. A. Farid and S. Hranilovic, "Capacity bounds for wireless optical intensity channels with Gaussian noise," *IEEE Trans. Inf. Theory*, vol. 56, no. 12, pp. 6066–6077, Dec. 2010.
- [7] A. Chaaban, J. Morvan, and M.-S. Alouini, "Free-space optical communications: capacity bounds, approximations, and a new sphere packing perspective," *IEEE Trans. Commun.*, vol. 64, no. 3, pp. 1176–1191, Mar. 2016.
- [8] R. Jiang, Z. Wang, Q. Wang and L. Dai, "A tight upper bound on channel capacity for visible light communications," *IEEE Communications Letters*, vol. 20, no. 1, pp. 97–100, Jan. 2016.
- [9] J. G. Smith, "The information capacity of amplitude- and variance constrained scalar Gaussian channels," *Inf. Contr.*, vol. 18, no. 3, pp. 203–219, Feb. 1971.
- [10] T. H. Chan, S. Hranilovic, and F. R. Kschischang, "Capacity-achieving probability measure for conditionally Gaussian channels with bounded inputs," *IEEE Trans. Inf. Theory*, vol. 51, no. 6, pp. 2073–2088, Jun. 2005.
- [11] R. You and J. M. Kahn, "Upper-bounding the capacity of optical IM/DD channels with multiple-subcarrier modulation and fixed bias using trigonometric moment space method," *IEEE Trans. Inf. Theory*, vol. 48, pp. 514–523, Feb. 2002.
- [12] S. Hranilovic, "Minimum-bandwidth optical intensity Nyquist pulses," *IEEE Trans. Commun.*, vol. 55, no. 3, pp. 574–583, Mar. 2007.
- [13] M. Tavan, E. Agrell, and J. Karout, "Bandlimited intensity modulation," *IEEE Trans. Commun.*, vol. 60, no. 11, pp. 3429–3439, Nov. 2012.
- [14] C. B. Czegledi, M. R. Khanzadi, and E. Agrell, "Bandlimited power-efficient signaling and pulse design for intensity modulation," *IEEE Trans. Commun.*, vol. 62, no. 9, pp. 3274–3284, Sept. 2012.
- [15] A. Lapidoth, *A Foundation in Digital Communication*, Cambridge University Press, 2009.
- [16] R. G. Gallager, *Information Theory and Reliable Communication*, New York: Wiley, 1968.
- [17] H. J. Landau, D. Slepian, and H. O. Pollack, "Prolate spheroidal wave functions, Fourier analysis and uncertainty III: The dimension of the space of essentially time- and band-limited signals," *Bell Syst. Tech. J.*, vol. 41, pp. 1295–1336, July 1962.
- [18] C. E. Shannon, "A mathematical theory of communication," *Bell Syst. Tech. J.*, vol. 27, pp. 379–423 and pp. 623–656, July and Oct. 1948.
- [19] N. C. Beaulieu and M. O. Damen, "Parametric construction of Nyquist-I pulses," *IEEE Trans. Commun.*, vol. 52, no. 12, pp. 2134–2142, Dec. 2004.
- [20] S. Shamai (Shitz), "On the capacity of a Gaussian channel with peak power and bandlimited input signals," *Archiv für Elektronik und Übertragungstechnik (AEÜ)*, vol. 42, no. 6, pp. 340–346, Nov.-Dec. 1988.
- [21] D. Middleton, *An Introduction to Statistical Communication Theory*, Institute of Electrical and Electronics Engineers, New York: McGraw-Hill, 1960.
- [22] G. D. Forney and G. Ungerboeck, "Modulation and coding for linear Gaussian channels," *IEEE Trans. Inf. Theory*, vol. 44, no.6, pp. 2384–2415, Oct. 1998.
- [23] T. Cover and J. A. Thomas, *Elements of Information Theory*, 2nd ed., John Wiley & Sons, Inc., 2006.